

# An inductive-capacitive-circuit-based micro-electromechanical system wireless capacitive pressure sensor for avionic applications: Preliminary investigations, theoretical modelling and simulation examination of newly proposed methodology

Measurement and Control  
2019, Vol. 52(7-8) 1029–1038  
© The Author(s) 2019  
Article reuse guidelines:  
sagepub.com/journals-permissions  
DOI: 10.1177/0020294019858095  
journals.sagepub.com/home/mac  


Sumit Kumar Jindal<sup>1</sup> , Ankush Mahajan<sup>2</sup> and Sanjeev Kumar Raghuvanshi<sup>2</sup>

## Abstract

Pressure is a key unit of measure in aerospace industries. Spontaneous precise measurement of pressure has to be compassed at locations where it is futile and impractical to couple the pressure responsive constituent to the conditional electronics or computational circuit by practicing standard cables and measurements prone to harsh environment. This paper introduces the design of a wireless pressure-monitoring system for aerospace applications in harsh environment. Traditionally, applied pressure deflects a delicate silicon diaphragm, altering the capacitance developed between it and metal electrode firm on a substrate. The LC circuit translates the pressure variation into the LC resonant frequency shift. This change is sensed remotely by virtue of inductance coupling, expelling the compulsion for wire connection rooted telemetry circuits. Novelty of our work rests in the fact that contrary to examining shift in the resonant frequency due to the applied pressure, we have put in effort to maintain resonant shifting equal to zero by varying the capacitance at the observer unit. This will allow pressure variations to be measured directly in terms of the capacitance variation at a fixed resonant frequency, which is 7.92 MHz in our context. According to the application domain (avionics), the proposed sensor structure is designed for functioning in the pressure range between (100 and 1140) mbar. The choice of design values for sensor parameters has been validated. The sensitivity is measured to be  $1.746e-17$  F/Pa over specified linear range which is shown to match a theoretical estimate realized by mathematical model. An in-depth, step by step derivation of performance parameters to achieve above-stated objective is shown for sensor under study. The results generated are modelled and examined using MATLAB. The analysis conducted dovetail perfectly with the modelled results.

## Keywords

Wireless sensor, sealed micro-electromechanical system capacitive sensor, pressure measurement, sensitivity, reflected impedance, inductor-gyrator

Date received: 17 July 2017; accepted: 2 May 2019

## Introduction

For a few but prominent industries such as aerospace, automotive and biomedical applications, a pivotal entity for calculation in a system is pressure.<sup>1–3</sup> Accurate and instantaneous determination of pressure is essential at remote locations where it is impossible to plant a measurement circuit by using recognized cable links. Accordingly, an integrated passive sensor capable of measuring pressure in severe environments such as high loading or high temperature is usually desired.<sup>4,5</sup>

Wireless passive sensors are one of the major sections in plenty of non-contact measurement

<sup>1</sup>School of Electronics Engineering, Vellore Institute of Technology, Vellore, India

<sup>2</sup>Department of Electronics Engineering, Indian Institute of Technology (Indian School of Mines), Dhanbad, India

### Corresponding author:

Sumit Kumar Jindal, School of Electronics Engineering, Vellore Institute of Technology, Vellore 632014, Tamil Nadu, India.  
Email: sumitjindal08@gmail.com



Creative Commons CC BY: This article is distributed under the terms of the Creative Commons Attribution 4.0 License (<http://www.creativecommons.org/licenses/by/4.0/>) which permits any use, reproduction and distribution of the work without

further permission provided the original work is attributed as specified on the SAGE and Open Access pages (<https://us.sagepub.com/en-us/nam/open-access-at-sage>).

applications.<sup>6</sup> One of the elementary varieties of wireless passive sensors is an inductive coupling resorted LC resonator.<sup>7,8</sup> Standard quality factor  $Q$  of this type of resonators is around 40.<sup>9</sup> By the reason that an LC passive pressure sensor does not require an internal power supply and a wire link, they have been extensively employed in some specialized applications.<sup>10</sup> Few of the industrial applications of the LC resonator-based sensor involve the systems for non-contact structural monitoring of concrete structures, sensing of intra-ocular pressure, pH monitoring, measurement of humidity, patient health monitoring, bio-potential measurement and strain monitoring of automobile tyre.<sup>7</sup> A conventional wireless passive LC sensor system has two magnetically coupled coils. One of the coils, named as sensor coil, is allied to a capacitive sensor and forms an LC tank circuit, whereas the second coil, called as observer coil, is electrically linked to a measurement circuit. The resonance frequency of the tank circuit is a function of variation in capacitance of the capacitive sensor. The external pressure results in the change of capacitance, so the sensor's resonant frequency alters. The value of applied pressure can be estimated from the frequency that can be remotely detected by another inductively coupled coil that is connected to the measurement circuitry.<sup>11</sup> Most of the existing methodology identifies the corresponding shift in resonance frequency utilizing suitable readout electronics and an impedance analyser.

Micro-electromechanical system (MEMS) capacitive pressure sensors are favoured for less weight, low cost, more reliability, smart functions, occupies very less space, low-power and telemetric applications since they never draw DC power and efficiently form passive inductor-capacitor (L-C) tank circuits for frequency-based measurement of pressure. Micromachined capacitive pressure sensors typically use an elastic diaphragm with fixed edges and a sealed cavity in between the diaphragm and the substrate below.<sup>12-14</sup>

This research explores a capacitive pressure sensor that consists of two micro machined metal plates with a gap depth. The capacitance change on application of pressure can be interrogated by varying the capacitance at the observer unit, keeping resonant shift constant. As always, the tank can be formed by coupling an inductor coil with the sensor separately, or it can be done by winding an insulated wire directly on the

sensor. The wireless interrogation can be implemented using an inductor that is magnetically coupled with the L-C tank device. This paper is constituted as follows. Section 'Transduction mechanism of capacitive pressure sensor' describes the transduction mechanism of capacitive pressure sensor. The details of the design of sensing unit are presented in section 'Design of sensing unit'. Section 'Circuit design for Si wireless module at observer unit' deals with circuit design for silicon wireless module at observer unit. The simulation results are evaluated in conjunction with the theoretical analysis in sections 'Sensitivity – major performance parameter' and 'Design specifications and considerations,' followed by discussion in section 'Preliminary investigations by simulations and interpretations'. Section 'Conclusion and future work' concludes the overall effort.

### Transduction mechanism of capacitive pressure sensor

The sensor depends upon the applied pressure which alters the distance separating the two electrodes, resulting in change of capacitance as shown in Figure 1. The clamped edge circular diaphragm used here operates as a capacitor with air as dielectric between them. Typically, bottom electrode is fixed and upper electrode is movable. The fundamental design comprises one silicon<sup>15,16</sup> membrane acting as movable electrode and another thin film electrode glass plate acting as a fixed electrode.<sup>17-21</sup> Electrodes are distant by a small gap which admits membrane deflection. Even in harsh environment,<sup>22</sup> the capacitance variation is sensed precisely and is allowed wireless transmission using an inductively coupled tank circuit having inherent resistance due to the inductor. According to the application field (avionics), the proposed sensor structures are designed for operating in the pressure range of (100–1140) mbar. This capacitance-based pressure sensor shows high linear pressure measurements which are important for avionics applications.<sup>23</sup>

### Design of sensing unit

The overall pressure sensing unit primarily has two aspects. First is pressure to deflection measurement and then deflection to capacitance measurement.

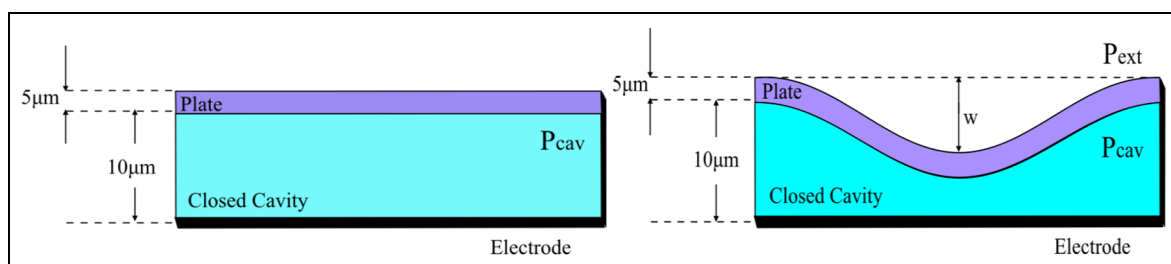


**Figure 1.** Clamped edge circular diaphragms with thickness  $5\ \mu\text{m}$  each and air gap of  $10\ \mu\text{m}$  working as a capacitor (left) under no pressure (right) under pressure.

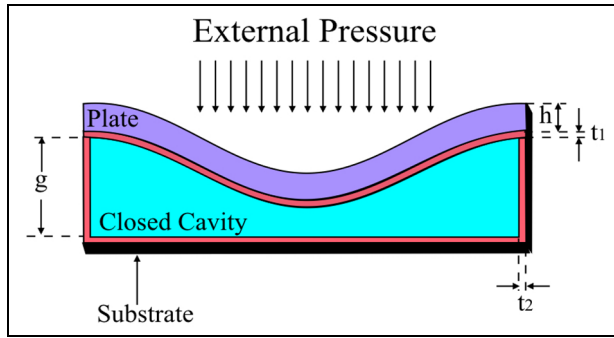


**Figure 2.** Mechanical capacitive principle of variable capacitor.

**Pressure to displacement variation**

Under consideration is diaphragm as a uniformly loaded circular plate with thickness  $h$ . Young’s modulus  $E$  and Poisson’s ratio  $\nu$  are the mechanical properties of the plate (Figure 2).

The geometry of the structure and the material properties of the MEMS capacitive pressure sensor for the deflection  $w(r)$  of an edge-clamped deflectable diaphragm under an applied pressure as a function of radius for  $(0 < r < a)$  is given by equation (1)<sup>14</sup>

$$w(r) = \frac{P(a^2 - r^2)^2}{64D} \tag{1}$$

where  $P$  is the applied pressure,  $a$  is the radius of the plate and  $r$  is the radial distance from the centre. At centre point of the plate the maximum centre deflection  $w_0$  occurs, that is, at  $(r = 0)$  and is given as follows<sup>14</sup>

$$w(0) = \frac{Pa^4}{64D} \tag{2}$$

where  $D$  is the flexural rigidity of the plate

$$D = \frac{Eh^3}{12(1 - \nu^2)} \tag{3}$$

**Analytical capacitance modelling and calculations**

Next to deflection of diaphragm is measure of equivalent capacitance variation between the two electrodes of the sensor. We know that the basic equation for capacitance of a parallel plate capacitor is given as<sup>22</sup>

$$C = \frac{A\epsilon_0\epsilon_r}{d} \tag{4}$$

where  $A$  is the area of circular parallel plates,  $d$  is the separation gap between the plates,  $\epsilon_r$  is the relative permittivity of dielectric material between the plates and  $\epsilon_0$  is the permittivity of free space.

On application of pressure, deflection is produced on the upper plate, which in turn decreases the gap between the clamped diaphragms. The capacitance change is proportional to the variation in the applied pressure which directly is a measure of change in the

gap from  $d$  to  $d - w(r, \theta)$ , where  $w(r, \theta)$  is the deflection in the upper diaphragm due to applied pressure. Small portion of area of diaphragm for small centre deflection can be obtained as follows

$$dA = r dr d\theta$$

The total capacitance due to the applied pressure can be calculated by integrating the area from  $r$  equal to 0 to radius and  $R$  and  $\theta$  equal to 0 to  $2\pi$  which is

$$C_{cd} = \epsilon \int_0^{2\pi} \int_0^R \frac{r dr d\theta}{d - w(r, \theta)} \tag{5}$$

Since the deflection on the diaphragm does not affect by the angle changes,  $w(r, \theta)$  can be replaced by  $w(r)$ . Finally, equation (5) can be obtained as follows

$$C_{cd} = \epsilon \int_0^{2\pi} \int_0^R \frac{r dr d\theta}{d - w(r)} \tag{6}$$

which can be further solved to get the following expression

$$C_{cd} = 8\pi\epsilon \sqrt{\frac{D}{Pd}} \tanh^{-1} \left( \frac{r^2}{8} \sqrt{\frac{P}{Dd}} \right) \tag{7}$$

Equation (7) shows the deflection to capacitance relation in terms of applied pressure, separation gap and flexural rigidity. The challenge here is the calculation of relative capacitance change, that is, changes in the capacitance relative to the capacitance obtained at zero applied pressure condition. With the mathematical formulation above, the obtained capacitance for the above clamped diaphragm geometry at zero pressure is 0.174 pF.

**Circuit design for Si wireless module at observer unit**

An  $LC$  sensor is typically designed from a spiral inductor linked with a sensing capacitor, forming a resonant  $LC$  tank. The capacitor changes in response to the parameter of interest, resulting in a shift in its resonant frequency. As an extension to the well-known literature, a new concept has been formulated, simulated and interpreted for pressure sensing. The sensor is modelled with an inductor  $L$  and a series resistance of the inductor  $R$  and a variable capacitance  $C$ . The resonance frequency of the sensor is given as follows<sup>7</sup>

$$\frac{1}{2\pi\sqrt{LC}} \tag{8}$$

Equivalent impedance for circuit leads to the inductance value of  $L = CR^2$ . A schematic representation of the typical  $LC$  sensor is exhibited in Figure 3 (left), and the corresponding equivalent impedance circuit is shown in Figure 3 (right).

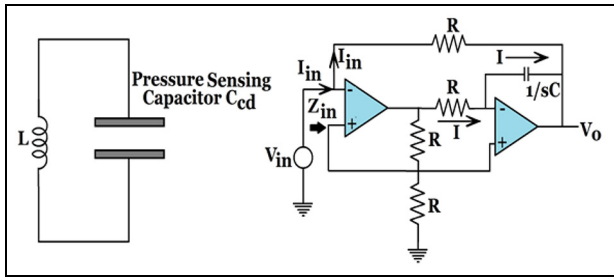


**Figure 3.** (Left) Simple LC circuit containing pressure sensing capacitor. (Right) Equivalent impedance of circuit leads to simulation of inductor-gyrator.

Instead of single tank circuit, inductively coupled tank circuit is used for wireless operation of the proposed design at the observer unit. The change in the resonant frequency occurring due to fractional change in capacitance in response to applied pressure is detected remotely by use of external coupled circuit called the observer unit. Using inductive coupling, the external coil energizes the sensor circuit which supplies load impedance that is reflected back to the impedance coil. Reflected impedance of coupled circuit is used for the wireless transfer of impedance of sensor unit to observer unit. Since there is no pre requisite of power source and wire connection in the sensing unit, the proposed design can be used in harsh environment with high reliability.

### Working principle and mathematical analysis

The practical method to sense the capacitance change due to applied pressure through inductively coupled arrangement is shown in Figure 4. Let  $C_s$  be the capacitance of the prime sensor on zero applied pressure. The air gap between the upper and lower diaphragm plate is  $10\ \mu\text{m}$ . At zero applied pressure, no deflection occurs and sensors initial capacitance is  $0.174\ \text{pF}$ . Theoretical resonant frequency of sensor at zero pressure is  $7.92\ \text{MHz}$ . Traditionally, when the sensor is under pressure, the capacitance changes and thus the sensor's resonant frequency also changes which can be registered with the reader unit. Researcher here has proposed the idea – what if we make shifting of resonant frequency equal to zero by varying capacitance at the observer unit? By and large the sensing unit experiences change in capacitance as soon as pressure is applied on upper plate of sensing capacitor. This induces a change in capacitance resulting in shift in of resonant frequency from  $7.92\ \text{MHz}$ . We have tried to work out a strategy to get back this change in resonant frequency to  $7.92\ \text{MHz}$  by varying capacitance at the observer unit. This allows us to directly sense the applied pressure in terms of capacitance at primary observer unit-wirelessly. The proposed methodology is in complete agreement for sensing of applied pressure in range of

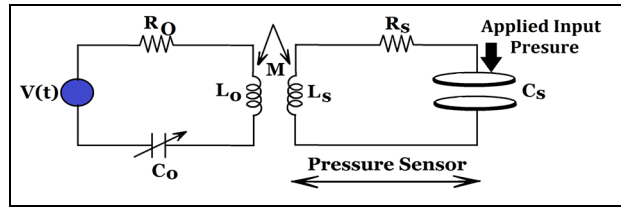


**Figure 4.** Electrical representation of the wireless measurement set-up with the L-C tank device illustrating both sensor and observer unit with inductively coupled coils  $L_0$  and  $L_s$  and 'M' as mutual inductance.

(100–1140) mbar used for avionic applications. Simulation results in section 'Preliminary investigations by simulations and interpretations' aid to novelty above.

For the design in Figure 4, the integral differential equations are as follows

$$V(t) = L_0 \frac{dI_0(t)}{dt} + R_0 I_0(t) + \frac{1}{C_0} \int_{-\infty}^t I_0(\tau) d\tau + M \frac{dI_s(t)}{dt} \quad (9)$$

$$0 = L_s \frac{dI_s(t)}{dt} + R_s I_s(t) + \frac{1}{C_s} \int_{-\infty}^t I_s(\tau) d\tau + M \frac{dI_0(t)}{dt} \quad (10)$$

Manipulating the above two equations in frequency domain and on proceeding with Fourier transform with initial conditions to be zero is given by

$$V(\omega) = L_0 j\omega I_0(\omega) + R_0 I_0(\omega) + \frac{1}{j\omega C_0} I_0(\omega) + M j\omega I_s(\omega) \quad (11)$$

$$0 = L_s j\omega I_s(\omega) + R_s I_s(\omega) + \frac{1}{j\omega C_s} I_s(\omega) + M j\omega I_0(\omega) \quad (12)$$

Conversely

$$\begin{aligned} V(\omega) &= \left( j\omega L_0 + R_0 + \frac{1}{j\omega C_0} \right) I_0(\omega) + j\omega M I_s(\omega) \\ &= Z_0(\omega) I_0(\omega) + j\omega M I_s(\omega) \end{aligned} \quad (13)$$

$$\begin{aligned} 0 &= \left( j\omega L_s + R_s + \frac{1}{j\omega C_s} \right) I_s(\omega) + j\omega M I_0(\omega) \\ &= Z_s(\omega) I_s(\omega) + j\omega M I_0(\omega) \end{aligned} \quad (14)$$

In general

$$Z_i(\omega) = j\omega L_i + R_i + \frac{1}{j\omega C_i} \quad (15)$$

for  $i = 'o'$  and  $'s'$ , that is, observer and sensing units, respectively

Further solution for  $I_0(\omega)$  and  $I_s(\omega)$  leads to

$$I_0(\omega) = \frac{Z_s(\omega)}{Z_s(\omega)Z_0(\omega) - (j\omega M)^2} V(\omega) \quad (16)$$

$$I_s(\omega) = -\frac{j\omega M}{Z_s(\omega)Z_0(\omega) - (j\omega M)^2} V(\omega) \quad (17)$$

From equations (16) and (17), one can state that resonance occurs at two frequencies.

For zero pressure condition;  $L_0 = L_s = L'$ ,  $R_0 = R_s = R'$  and  $C_0 = C_s = C'$  which leads to  $Z_s(\omega) = Z_0(\omega)$ .

For getting resonant frequencies by accrediting the denominator equal to zero in equations (16) and (17), we obtain

$$\omega_1^2 = \frac{1}{L'C'(1 - \frac{M}{L})} \quad (18)$$

$$\omega_2^2 = \frac{1}{L'C'(1 + \frac{M}{L})} \quad (19)$$

$$\kappa = \frac{M}{L} \quad (20)$$

where equation (20) is the coupling coefficient.<sup>24</sup>

In contrast to simple tank circuit, here we achieve two resonant frequencies shifted by a measure of  $1/1 \pm \kappa$ . The equivalent primary impedance  $Z_{eqp}$  is obtained by solving equations (9) and (10)

$$Z_{eqp} = \frac{V}{I_s} = Z_0 - \frac{Z_M^2}{Z_s} \quad (21)$$

where  $Z_M = j\omega M$

## Sensitivity – major performance parameter

### Capacitive sensitivity

Capacitive sensitivity of the capacitive pressure sensor can be defined as the ratio of change in capacitance to the fractional change in the applied pressure, numerically defined as

$$S_{cap} = \frac{\partial C_{cd}}{\partial P} \quad (22)$$

This ultimately leads to

$$S_{cap} = 0.2419 \frac{\epsilon(1 - \nu^2)r^6}{Ed^2h^3} \quad (23)$$

For the proposed design, capacitive sensitivity is calculated to be  $1.746e-17$  F/Pa which is desirable for MEMS design for application under consideration.

### Mechanical sensitivity

Mechanical sensitivity is defined as the ratio of deflection of diaphragm obtained with respect to applied pressure, that is

$$S_{mec} = \frac{w}{P} \quad (24)$$

Using the parameters and working out the expression lead to

$$S_{mec} = \frac{0.1875r^4(1 - \nu^2)}{Eh^3} \quad (25)$$

## Design specifications and considerations

First, the outline dimensions are defined. Within the given frame, the cavity supporting structure is constructed. The geometry confided upon the necessary pressure range to be sensed and provided assembling settings. In most cases, a sensor for high-pressure sensing necessitates rigid supporting structure. When the membrane size is decided, the gap is figured out first from the mathematics of capacitor calculation, and then a simulation is performed using the proposed geometry. The design is optimized using simulations. To mention, an MEMS capacitive pressure sensor (as shown in Figure 2) with 10- $\mu$ m air gap, 250- $\mu$ m membrane radius and 5- $\mu$ m electrodes/membrane thickness has been selected for primary sensing.

The tank is built by coupling an inductor coil with the sensor independently; else, it can be formed by winding an insulated wire precisely on the sensor as shown in Figure 5. The wireless interrogation can be realized utilizing an inductor that is magnetically coupled with the L-C tank. Specification for design of sensor is summarized in Table 1.

## Preliminary investigations by simulations and interpretations

In Figure 6, variation of surface deflection with radius of circular diaphragm is investigated at a pressure of 0.5 bar. Equations (1)–(3) are used to simulate this result. Performance is investigated for  $P = 0.5$  bar,  $r = 180$   $\mu$ m,  $E = 170 \times 10^9$  N/m<sup>2</sup> and  $\nu = 0.28$ . It is observed that diaphragm deflection is maximum at the

**Table 1.** Structural parameters for the sensor.

Parameters	Design value
Young's modulus, $E$	$170 \times 10^9$ N/m <sup>2</sup>
Thickness, $h$	5 $\mu$ m
Gap depth, $d$	10 $\mu$ m
Poisson's ratio for silicon, $\nu$	0.28
Radius of diaphragm, $a$	250 $\mu$ m
Applied pressure range, $P$	(100–1140) mbar
Sensor nominal capacitance at zero applied pressure, $C_s$	0.174 pF
Observer inductance, $L_0$	4.35 mH
Sensor inductance, $L_s$	4.35 mH
Observer resistance, $R_0$	4 k $\Omega$
Sensor resistance, $R_s$	4 k $\Omega$

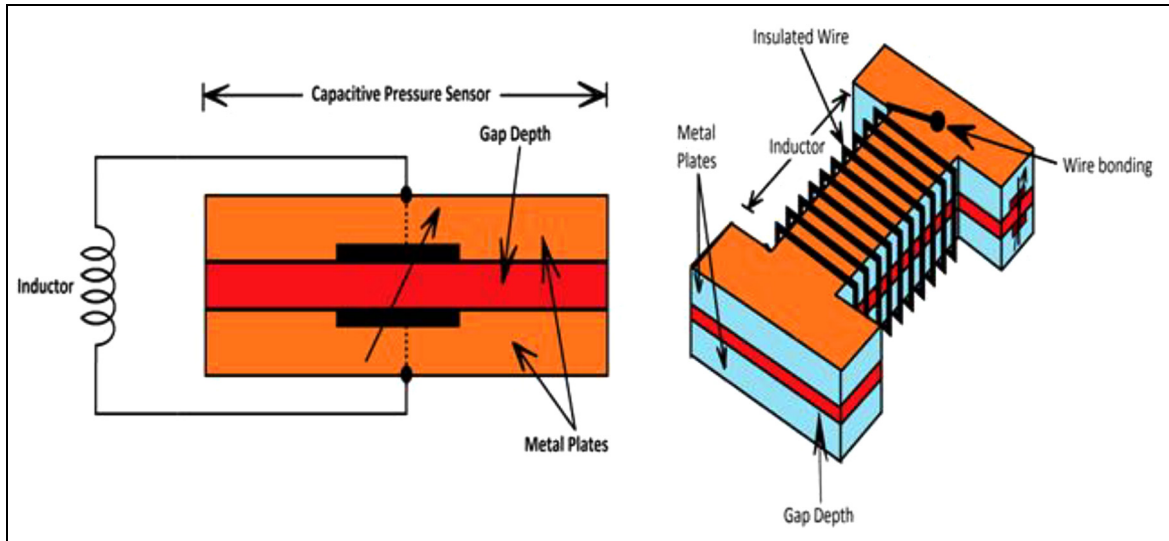


**Figure 5.** MEMS capacitive pressure sensor with L-C tank arrangement for capacitance-based pressure detection. (Left) Cross-sectional view of the sensor coupled with a separate inductor. (Right) Device with an inductor wound on the sensor.

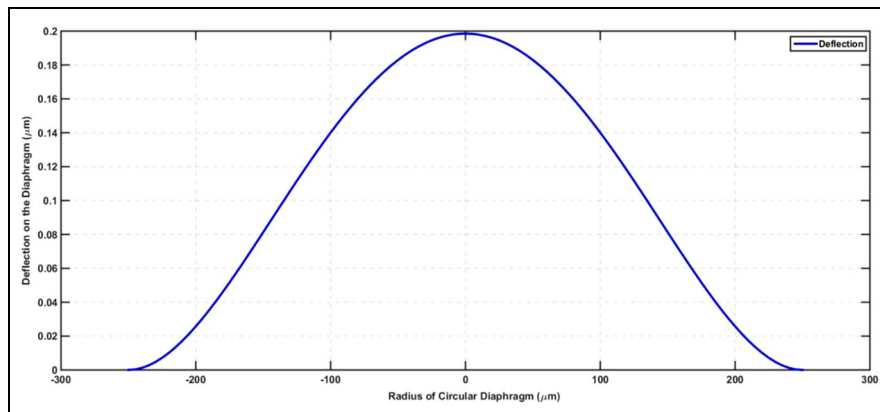


**Figure 6.** Variation of surface deflection with radius of circular diaphragm at a pressure of 0.5 bar.

centre and is equal to  $0.2 \mu\text{m}$  and it decreases as radius increases. The data belong to the sensor side. The variation of surface deflection with radius of circular diaphragm is compared with work done in Jindal et al.<sup>14</sup> The comparison of proposed design with stated cross-reference is valid since the value of structural parameters has been taken from previous works.<sup>14,21</sup> Deflection of the diaphragm in both the schemes increases initially till it reaches a peak and then settles down gradually as radius of diaphragm increases.

In Figure 7, relative capacitance change for the designated pressure range, that is, 0.1–1.14 bar is under investigation. Equation (7) is used to simulate this result. Performance is investigated for  $P = (100\text{--}1140) \text{ mbar}$ ,  $r = 180 \mu\text{m}$ ,  $E = 170 \times 10^9 \text{ N/m}^2$  and  $\nu = 0.28$ . Zero pressure capacitance is observed to be  $0.174 \text{ pF}$ . It is evident that capacitance variation is near about linear. Hence, it can be interpreted that proposed methodology can precisely measure pressure to 1.14 bars satisfying crucial obligations for avionics

applications. The data belong to the sensor side. The relative capacitance change is compared with work done in Jindal and colleagues.<sup>14,22</sup> Here, since the pressure range is low, the simulated graph shows a linear response throughout. In Jindal and colleagues,<sup>14,22</sup> pressure range in normal mode is  $(0\text{--}0.2) \text{ MPa}$  and hence we received a non-linear response.

In Figure 8, resonant frequency points are under discussion. At resonance, the output is reduced due to the resistive reflected impedance, which tries to lower the quality factor of the primary. To enhance the performance of the output, the coupling must be compensated. We get inductive reflected impedance at frequencies lower than the exact resonance point, which produces a peak at the output and we get capacitive reflected impedance at frequencies higher than exact resonance point, which results in another peak in the output. Performance is investigated for  $P = (100\text{--}1140) \text{ mbar}$ ,  $r = 180 \mu\text{m}$ ,  $E = 170 \times 10^9 \text{ N/m}^2$ ,  $\nu = 0.28$ ,  $L_0 = 4.35 \text{ mH}$ ,  $L_s = 4.35 \text{ mH}$ ,  $R_0 = 4 \text{ k}\Omega$  and  $R_s = 4 \text{ k}\Omega$ .

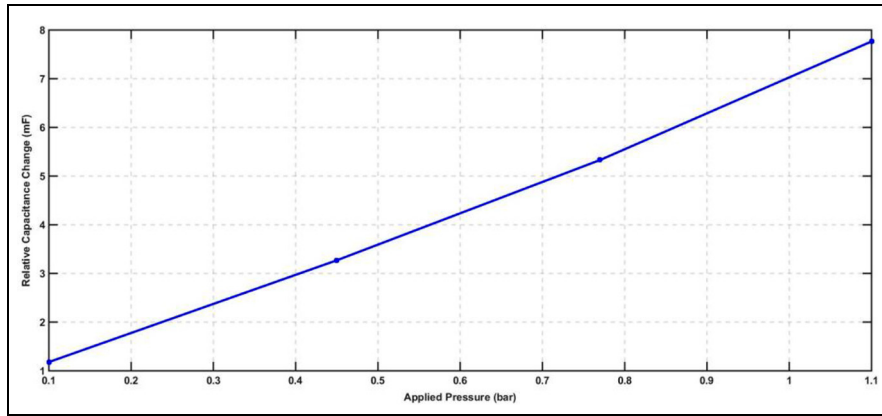


Figure 7. Relative capacitance variation with respect to zero pressure condition.

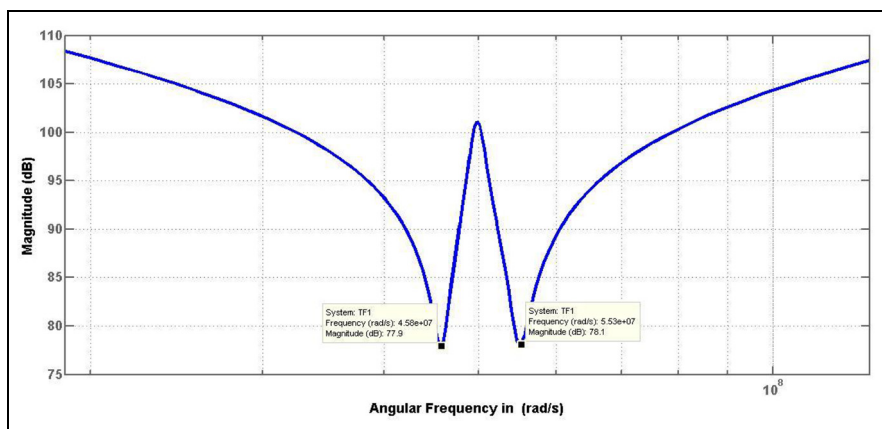


Figure 8. Resonant frequency points at two angular frequencies for proposed design at  $4.55 \times 10^7$  rad/s and  $5.53 \times 10^7$  rad/s.

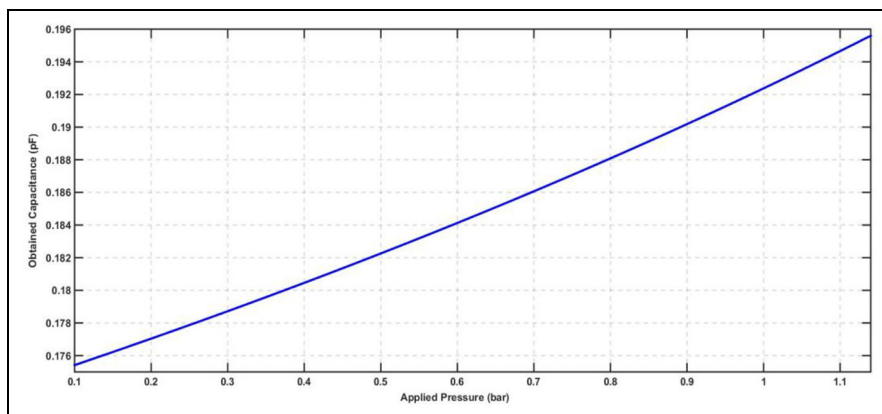
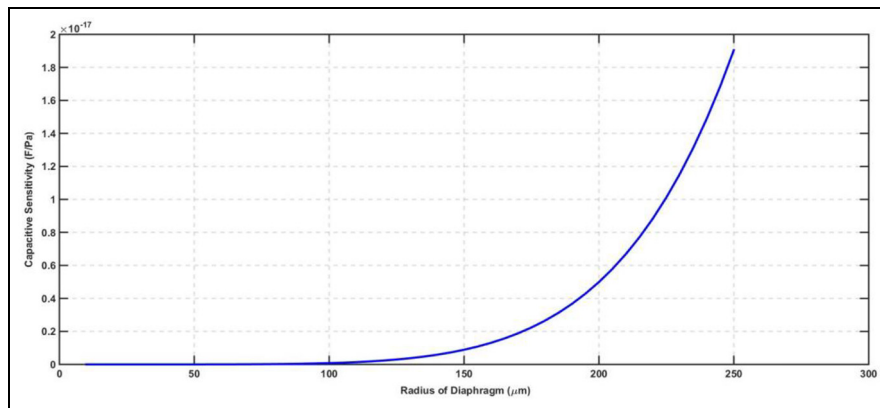


Figure 9. Final capacitance variation at primary observer unit to sense the applied pressure range.

Figure 8 is a result of simulating equations (13) and (14). Resonant frequency points at two angular frequencies for proposed design are  $4.55 \times 10^7$  rad/s and  $5.53 \times 10^7$  rad/s. The data belong to the observer side.

As a solution to above, if we make capacitance at observer unit variable (wireless control) and vary it to such a degree that even under pressure resonant

frequency doesn't shift, then we can sense applied pressure in terms of capacitance for the desired range of (100–1140) mbar. In Figure 9, capacitance variation at primary observer unit to sense the applied pressure range is investigated. Figure 9 is a result of simulating equation (2) with applied pressure against obtained capacitance. Performance is investigated for  $P = (100-$



**Figure 10.** Variation of capacitive sensitivity with the variation in the diaphragm radius at a fixed thickness and pressure.

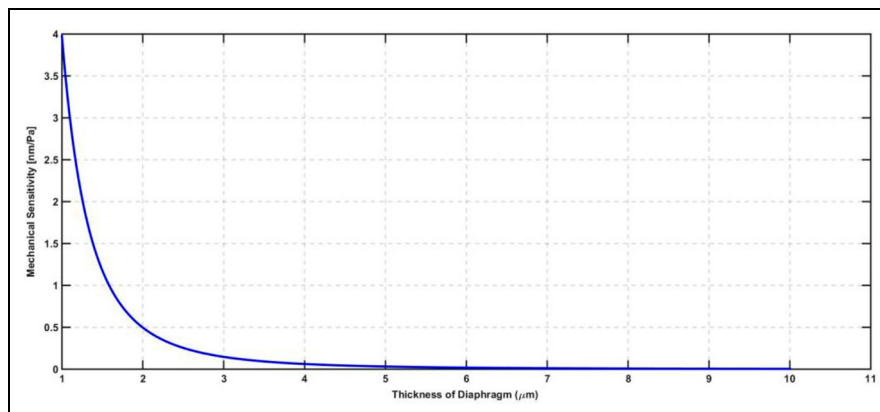


**Figure 11.** Variation of mechanical sensitivity with the variation in the diaphragm thickness at a fixed radius and pressure.

1140) mbar,  $r = 180 \mu\text{m}$ ,  $a = 250 \mu\text{m}$ ,  $E = 170 \times 10^9 \text{ N/m}^2$  and  $\nu = 0.28$ . It can be observed that minimum capacitance at 100 mbar is 0.174 pF and maximum obtained capacitance is 0.196 pF at 1140 mbar. The data belong to the observer side. The capacitance variation at primary observer unit to sense the applied pressure range is compared with work done in previous works.<sup>14,21</sup> Here, since the pressure range is low, the simulated graph shows a linear response throughout. In Jindal and colleagues<sup>14,21</sup>, pressure range in normal mode is (0–0.2) MPa and hence we received a non-linear response. Moreover, response in Jindal and colleagues<sup>14,21</sup> is extended to touch mode of the sensor for pressure range of (0.2–2) MPa. Highly non-linear response can be observed since the pressure range is very high.

Figure 10 shows the variation of the capacitive sensitivity with respect to the variation in the radius of the circular diaphragm. Figure 10 is a result of simulating equation (23) with radius of diaphragm against capacitive sensitivity of proposed sensor. Performance is investigated for  $d = 10 \mu\text{m}$ ,  $h = 5 \mu\text{m}$ ,  $r = 180 \mu\text{m}$ ,  $a = 250 \mu\text{m}$ ,  $E = 170 \times 10^9 \text{ N/m}^2$  and  $\nu = 0.28$ . It illustrates that with the increase in the radius of diaphragm at a fixed thickness and uniform pressure, the deflection on the circular diaphragm increases. Validating a

design consideration from Figure 10, we can justify the choice of having radius for our sensor design to be  $250 \mu\text{m}$ . At this geometry of diaphragm radius at a fixed thickness of  $5 \mu\text{m}$ , the variation in the above plot is almost constant. The data belong to the sensor side. The variation of the capacitive sensitivity with respect to the variation in the radius of the circular diaphragm is compared with the work done in Jindal et al.<sup>14</sup> The response curve and inference in both the cases are same, but the magnitude of capacitive sensitivity is different because value of gap depth chosen is different.

In Figure 11, variation of the mechanical sensitivity analogous to the variation in the diaphragm thickness is investigated. Figure 11 is a result of simulating equation (25) with thickness of diaphragm with mechanical sensitivity. Performance is investigated for  $h = 5 \mu\text{m}$ ,  $r = 180 \mu\text{m}$ ,  $E = 170 \times 10^9 \text{ N/m}^2$  and  $\nu = 0.28$ . It can be concluded from Figure 11 that with the increase in diaphragm thickness, the mechanical sensitivity decreases. This is because with the increase in diaphragm thickness, deflection decreases. The data belong to the sensor side. Another claim to validation of chosen geometry is the choice of diaphragm thickness. Beyond  $5 \mu\text{m}$  if the thickness is further increased, the mechanical sensitivity drops by a considerable amount which is inadmissible. The variation of mechanical

sensitivity analogous to the variation in the diaphragm thickness is compared with the work done in Jindal et al.<sup>14</sup> The response curve and inference in both the cases are same, but the magnitude of mechanical sensitivity is different because the value of radius of diaphragm chosen is different.

## Conclusion and future work

This research has explored a unique methodology for LC tank circuit-based wireless MEMS capacitive pressure sensor which can measure applied pressure by changing the capacitance and keeping frequency shift constant. Sections ‘Introduction’ and ‘Transduction mechanism of capacitive pressure sensor’ introduced the concept of wireless sensing using LC tank circuit with proper insight to literature review. Since capacitive pressure sensor is a vital member of the design, the transduction mechanism for this sensor has been elucidated in ample capacity. Next, two sections delineate in depth the step-by-step theoretical evaluation of crucial parameters. Section ‘Preliminary investigations by simulations and interpretations’ delved into depth graphically analysing the methodology for the refined model and comparing the results with intuitive predictions. It was observed that the resulting capacitance variation on keeping frequency shift constant can also be used for passive measurement of applied pressure. The performance in sensitivity was also observed to be as per fondness and validity of avionic applications. The maximum sensitivity was observed to be  $1.746e-17$  F/Pa. The comparison between the simulation result and theoretical response obtained revealed the effectiveness of the model in predicting the sensor response. The presented methodology-based wireless Si MEMS is the first building block of a platform for autonomous industrial sensors and has all the essential characteristics necessary for integration into harsh industrial environments. The compact, single-substrate design leaves plenty of room for replacement of Si with SiC, operation of sensor in touch mode, as a future work for even better performance of target application.

## Declaration of conflicting interests

The author(s) declared no potential conflicts of interest with respect to the research, authorship and/or publication of this article.

## Funding

The author(s) received no financial support for the research, authorship and/or publication of this article.

## ORCID iD

Sumit Kumar Jindal  <https://orcid.org/0000-0002-9676-3541>

## References

1. Lin L and Yun W. MEMS pressure sensor for aerospace applications. In: *Proceedings of the IEEE aerospace conference*, Aspen, CO, 28 March 1998, pp. 429–436. New York: IEEE.
2. Hsu TR. *MEMS and microsystems design and manufacture*. New York: Tata McGraw Hill, 2002.
3. Pavlin M, Belavic D and Novak F. Ceramic MEMS designed for wireless pressure monitoring in the industrial environment. *Sensors* 2012; 12: 320–333.
4. Yang J. A harsh environment wireless pressure sensing solution utilizing high temperature electronics. *Sensors* 2013; 13: 2179–2734.
5. Rodriguez RI and Jia Y. A wireless inductive-capacitive (L-C) sensor for rotating component temperature monitoring. *Int J Smart Sens Intell Syst* 2011; 4(2): 325–337.
6. Takahata K and Gianchandani YB. A micromachined capacitive pressure sensor using a cavity-less structure with bulk-metal/elastomer layers and its wireless telemetry application. *Sensors* 2008; 8: 2317–2330.
7. Huang QA, Dong L and Wang LF. LC passive wireless sensors toward a wireless sensing platform: status, prospects, and challenges. *J Microelectromech Syst* 2016; 25(5): 822–841.
8. Han CH, Choi DH and Yoon JB. Parallel-plate MEMS variable capacitor with superior linearity and large tuning ratio using a leveraging structure. *J Microelectromech Syst* 2011; 20: 1345–1354.
9. Huixin Z, Yingping H, Binger G, et al. A readout system for passive pressure sensors. *J Semicond* 2013; 34(12): 125006.
10. Zhou M-X, Huang Q-A, Qin M, et al. A novel capacitive pressure sensor based on sandwich structures. *J Microelectromech Syst* 2005; 14(6): 1272–1212.
11. Hyeoncheol K, Jeong YG and Chun K. Improvement of the linearity of capacitive pressure sensor using an interdigitated electrode structure. *Sensor Actuat A Phys* 1997; 62: 586–590.
12. Bakhoum EG and Cheng MHM. Capacitive pressure sensor with very large dynamic range. *IEEE Trans Comp Pack Technol* 2010; 33(1): 79–83.
13. Jindal SK and Raghuvanshi SK. A complete analytical model for circular diaphragm pressure sensor with freely supported edge. *Microsyst Technol* 2014; 21(5): 1073–1079.
14. Jindal SK, Mahajan A and Raghuvanshi SK. A complete analytical model for clamped edge circular diaphragm nontouch and touch mode capacitive pressure sensor. *Microsyst Technol* 2015; 22(5): 1143–1150.
15. Pratap R and Kumar AA. Material selection for MEMS. *India J Pure Appl Phys* 2007; 45: 358–367.
16. Jindal SK and Raghuvanshi SK. Study of materials for the design of MEMS capacitive pressure sensor. *AIP Conf Proc* 2016; 1724: 020118.
17. Han J and Shannon MA. Smooth contact capacitive pressure sensors in touch- and peeling-mode operation. *IEEE Sens J* 2009; 9(3): 199–206.
18. Daigle M, Corcus J and We K. An analytical solution to circular touch mode capacitor. *IEEE Sens J* 2007; 7(4): 502–505.
19. Varma AP, Thukral D and Jindal SK. Investigation of the influence of double-sided diaphragm on performance of capacitance and sensitivity of touch mode capacitive

- pressure sensor: numerical modeling and simulation forecasting. *J Comput Electron* 2017; 16: 987–994.
20. Jindal SK, Mahajan A and Raghuwanshi SK. Reliable before-fabrication forecasting of normal and touch mode MEMS capacitive pressure sensor: modeling and simulation. *J Micro-Nanolith MEM* 2017; 16: 045001.
  21. Fragiaco G, Ansbeak T, Pedersen T, et al. Analysis of small deflection touch mode behaviour in capacitive pressure sensor. *Sensor Actuat A Phys* 2010; 161: 114–119.
  22. Jindal SK and Raghuwanshi SK. Capacitance and sensitivity calculation of double touch mode capacitive pressure sensor: theoretical modeling and simulation. *Microsyst Technol* 2016; 23(1): 135–142.
  23. Eswaran P and Malarvizhi S. Modeling and analysis of MEMS capacitive differential pressure sensor structure for altimeter application. *Microsyst Technol* 2017; 23: 1343–1349.
  24. Duarte RM and Felic GK. Analysis of the coupling coefficient in inductive energy transfer systems. *Active Passive Electron Comp* 2014; 2014: 951624.